Linear Diffusion Profiles due to Long Range Adsorbate Interactions: Cs/Si(100) at Low Coverage

R. H. Milne, M. Azim, R. Persaud, and J. A. Venables*
School of Mathematical and Physical Sciences, University of Sussex, Brighton BN1 9QH, United Kingdom

(Received 1 April 1994)

Diffusion of Cs on Si(100) was examined using biased secondary electron imaging, capable of detecting Cs coverages $\theta \geq 0.005$ ML. Unusual diffusion profiles, linear at low θ, with edges expanding as $t^{1/2}$, were obtained for $\theta < \frac{1}{2}$ ML. These results are modeled with a diffusion coefficient of the form $D \sim D_1 + D_2(A/kT)[\theta(1-\theta)]$. This form is consistent with diffusion theory including strongly repulsive Cs-Cs interactions, deduced from the decrease of the adsorption energy, $q(\theta)$, with coverage ($dq/d\theta \simeq -2$ eV/ML). Measurements of D in the range $60 \leq T \leq 90$ °C are consistent with an adatom diffusion energy, $E_d = 0.47 \pm 0.05$ eV.

PACS numbers: 68.35.Fx

The diffusion of adsorbed particles across crystalline surfaces plays an important part in their ordering at submonolayer coverages and is linked to adsorbate-substrate and adsorbate-adsorbate interactions. It is therefore a fundamental process in the growth of technologically important ultrathin films. The subject of surface diffusion of adsorbates has been reviewed several times [1–3]. The diffusion coefficient D, which in general is a function of coverage (θ) and temperature (T), contains valuable information about the nature of the diffusion process. In general, this coefficient can vary considerably depending on the nature and interactions of the adsorbate and substrate; however, information on these effects is still rather limited. In this Letter, we present results for the diffusion of Cs on Si(100)-(2 × 1), with particular emphasis on the coverage region $\theta < \frac{1}{6}$ of a monolayer (ML). Unusual linear diffusion profiles are obtained for this system. These are explained in terms of surface diffusion theory incorporating repulsive Cs interactions; some atomic parameters are deduced.

In our experiments, Cs was deposited at room temperature (RT) onto the silicon substrate through a mask, to form a series of patches with dimensions typically $\sim(0.1 \times 0.1)$ mm^2. As a consequence of the dramatic decrease in work function, there is a corresponding large increase in the secondary electron yield. This allowed us to detect the patches using biased secondary electron imaging (b-SEI) [4]. In fact, b-SEI exhibits a remarkable sensitivity for this system: Cs concentrations >0.02 ML can be readily detected with a high signal to noise ratio, implying that the detection sensitivity is <0.005 ML. The b-SEI contrast has been calibrated at coverages ≤0.5 ML, where the contrast is maximum, and has a value around 250% with respect to the background Si(100) signal [5]. Previous experiments compared the SE intensity from the center of patches with the signal from the clean Si for various deposition times. The coverage at maximum contrast was taken as $\theta = \frac{1}{2}$ ML, thus giving a calibration curve for converting SE contrast to coverage [5]. The SE line scans, obtained from the patches during the diffusion experiments, were converted into concentration profiles using this curve.

The initial profiles are fairly stable at room temperature (Fig. 1) and the substrate has to be heated to between 50–100 °C in order to observe appreciable diffusion. The temperature range is so limited in order to suppress effects of desorption. For initial coverages less than $\frac{1}{6}$ ML, the diffusion is essentially linear [Fig. 1(a)]. For higher coverages it is more complex [Fig. 1(b)]; however, the low concentration part remains fairly linear. The main purpose of this Letter is to consider the linear concentration profiles observed at low coverages.

The diffusion distance (Δx) is usually related to the diffusion coefficient (D) through the expression $\Delta x\,(2Dt)^{1/2}$ where D is often written as

$$D = D_0 \exp(Q/kT). \tag{1}$$

Q is the activation energy for diffusion, k is Boltzmann's constant, and D_0 the prefactor. As is expected from a

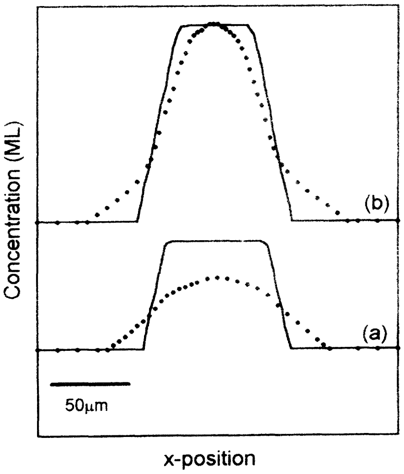

FIG. 1. Concentration profiles of initial deposits (solid lines) and after diffusion (dots); (a) 0.13 ML, (b) 0.23 ML.

0031-9007/94/73(10)/1396(4)$06.00

classical diffusion model, the expansion of the patches exhibited a linear relationship with the square root of time (Fig. 2). However, for coverages $\frac{1}{6} < \theta < \frac{1}{3}$ ML, the slope of the line was found to be almost independent of the initial concentration for the same substrate temperature. At higher, or lower, coverages the slopes are less steep. This, we contend, is due to repulsive interactions between the Cs adatoms in addition to the Cs overlayer structures, influencing the values of $D_0(\theta)$ and $Q(\theta)$ markedly.

These interactions also cause major changes in the heat of adsorption $q(\theta)$, which decreases strongly with θ in the same range. In the present work, values of $q(\theta)$ for Cs/Si(001)-2 × 1 have been obtained directly, by observing the change in surface concentration during thermal desorption. This was done by heating for $\Delta t = 1$ min at temperatures in the range $175 < T < 375$ °C and noting the concentration decrease from θ to $\theta_{\Delta t}$. Then, using the equation [6]

$$q(\theta) = -kT \ln[\ln(\theta/\theta_{\Delta t})/(\nu \Delta t)], \qquad (2)$$

the results shown in Fig. 3 were obtained; ν is an attempt frequency of the order of $10^{13}\,\mathrm{s}^{-1}$ at room temperature. The extrapolation to zero coverage gives $q_0 \sim 2$ eV and the initial slope, $dq/d\theta \sim -2$ eV/ML. There are changes in the slope at approximately $\frac{1}{6}$ and $\frac{1}{2}$ ML.

The diffusion experiments show several unusual features including the shape of the profiles and the similarity of Δx for patches which have substantially different initial concentrations. In order to understand these results, it is necessary to examine the structure of Cs on Si as a function of coverage.

The adsorption of alkali metals onto semiconductor surfaces has been extensively studied [7]. However, the adsorption structure, the nature of the chemical bond and surface metallization for many of these systems, including Cs/Si(100), remain controversial. Although the nature of the bonding is still subject to discussion, it is generally agreed that at low coverages, electron transfer between the adsorbate and the substrate results in the formation of dipoles which explain the dramatic decrease in the work function [8]. As the coverage increases, each dipole is subject to a depolarization arising from the electric field due to all the others, and the work function curve goes through a minimum before approaching the bulk value of the adsorbate. For $\theta < \frac{1}{2}$ ML, it has been proposed [9] that the Cs atoms occupy the pedestal sites (at the center of two silicon dimers). Low energy electron diffraction results, obtained at room temperature [10], show that there is a stable structure at $\frac{1}{6}$ ML with every third pedestal site occupied. No regular, stable structures were observed below this coverage. For coverages above $\frac{1}{6}$ ML, it is proposed that the next stable structure (at $\frac{1}{3}$ ML) consists of pairs of atoms on adjoining sites separated by one unoccupied site.

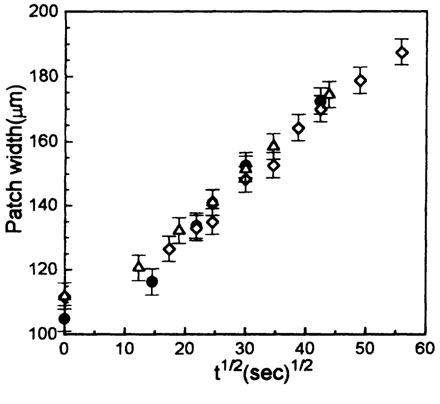

FIG. 2. Increase in patch width plotted against $t^{1/2}$ for three concentrations at 60 °C; (i) 0.13 ML (circles), (ii) 0.23 ML (diamonds), and (iii) 0.32 ML (triangles).

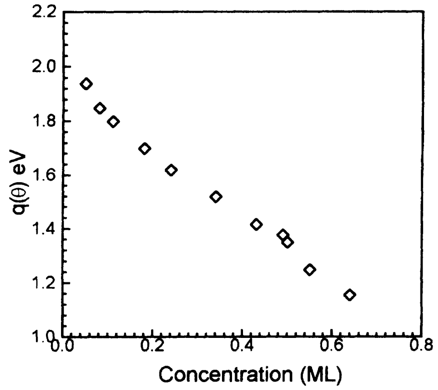

FIG. 3. The change of heat of adsorption with coverage, obtained from thermal desorption experiments.

These ideas can be used to interpret our results in a simple way. At or below $\frac{1}{6}$ ML, the adatoms are mostly separated by at least two unoccupied sites and the individual dipole moments are large, resulting in substantial dipole-dipole repulsion. Above $\frac{1}{6}$ ML some of the atoms are in adjoining sites where the repulsion is reduced due to depolarization. Indeed, it is possible that a precursor of metallic bonding [11] is present at these coverages. Our results indicate that it is the separated atoms that produce most of the observable diffusion, while the atoms in the more condensed areas dissociate and act as a source for the dilute phase. This simplified model helps to explain the enhanced diffusion at lower coverages and the similarity of the patch width vs $t^{1/2}$ plots for coverages $> \frac{1}{6}$ ML (in effect, the diffusing adatoms originate from a concentration of $\frac{1}{6}$ ML). Above $\frac{1}{3}$ ML the dissociation of pairs or chains of atoms becomes the rate limiting step and results in reduced diffusion.

The above argument deals qualitatively with the observed rate of diffusion but does not explain the linear nature of the diffusion profiles. First, we establish the

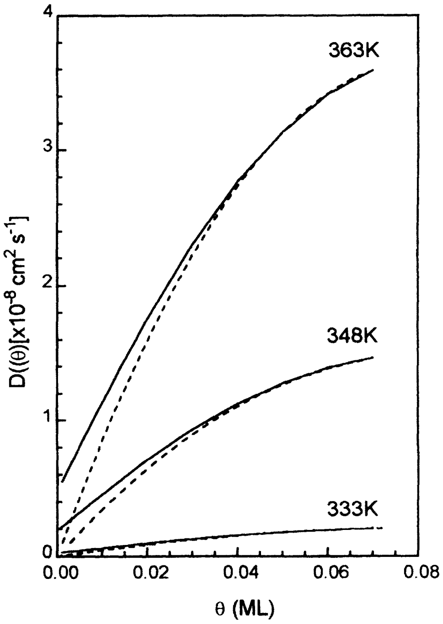

FIG. 4. Evaluation of $D(\theta)$ at three temperatures; (i) using the experimental parameters with Boltzmann-Matano analysis of a straight line profile (dashed lines) and (ii) thermodynamic calculations (solid lines).

form of $D(\theta)$ which gives an exact linear profile. Then we show that a similar form is obtained when the heat of adsorption decreases linearly and strongly with coverage. This form is then used in comparison with the experimental diffusion coefficients at three temperatures, and the Cs diffusion energy, E_d, is deduced.

Boltzmann and Matano in Ref. [2] showed that the coverage dependent diffusion coefficient $D(\theta)$, can be deduced from a concentration profile produced after time t, using the expression

$$D(\theta) = -\frac{1}{2t}\left[\frac{\partial x}{\partial \theta'}\right]\int_{\theta_0}^{\theta} x \, d\theta', \tag{3}$$

where x is the distance from the original step in the concentration profile. Assuming an initial step profile evolves to give a linear concentration gradient, and $\Delta x = (2D_1 t)^{1/2}$ is the distance moved by the edge of the patch, then Eq. (3) yields

$$D(\theta) = \frac{D_1}{\theta_1}[\theta(1 - C\theta)], \tag{4}$$

where θ_1 is half the initial concentration and $C = 1/2\theta_1$. Equation (4) represents the general form of the diffusion coefficient for a straight line profile. This can be understood as $(1 - C\theta)$ being the number of sites available to the diffusing atoms; the term in θ is due to the variation of (repulsive) adsorbate interactions with concentration. Note that if this form were really true down to $\theta = 0$, then isolated adatoms would not diffuse at all; this is hardly likely in practice. However, this $\theta(1 - C\theta)$ dependence emerges as the dominant term when strongly repulsive interactions are considered in terms of atomic mechanisms.

In the case of diffusion of noninteracting species, the diffusion coefficient is given by [2],

$$D = \Gamma(0)\lambda^2, \tag{5}$$

where λ^2 is the mean square jump distance, and $\Gamma(0)$, the jump frequency of adatoms along the x direction, given by absolute rate theory as

$$\Gamma(0) = \nu \exp(\Delta S_j/k)\exp(-E_d/kT). \tag{6}$$

ΔS_j is the activation entropy corresponding to the transition of an atom from a potential minimum to the saddle point and E_d is the activation energy for adatom diffusion. In the case of interacting adsorbate particles, diffusion is determined by the chemical potential gradient. It is enhanced towards regions where the binding energy is greater; for repulsive interactions this is towards lower coverages. This physical effect is accounted for by including the thermodynamic factor $[(\partial\mu/kT)/\partial\ln\theta]_T$ in D_0 [2], where μ is the chemical potential.

Repulsive interactions can also directly lower the activation barrier. The average concentration variation of this effect can be accounted for by including another exponential term [2,12]. Combining these terms with a $(1 - \theta)$ term (the number of available sites) gives an expression for the concentration dependent diffusion coefficient

$$D(\theta) = \nu \exp(\Delta S_j/k)\lambda^2(1 - \theta)\left[\frac{\partial\mu/kT}{\partial\ln\theta}\right]_T \exp\left(\frac{-Q}{kT}\right), \tag{7}$$

where now Q depends on E_d and $q(\theta)$ as

$$Q = E_d + \left(\frac{\partial\ln\theta}{\partial\mu}\right)_T\left(\frac{\partial[-q(\theta)]}{\partial\ln\theta}\right)_T.$$

For interacting particles μ can be approximated by

$$\mu = \mu^0 + kT\ln[\theta/(1 - \theta)] - q(\theta), \tag{8}$$

where μ^0 is the standard chemical potential.

To extend the analysis we now assume that $q(\theta)$ decreases linearly with θ at low coverages. This is a reasonable approximation for systems where large dipole moments are present at the onset of adsorption, for example, Cs/W(110) [13], Na/Si(001)-2 × 1 [6], and our own results (Fig. 3). Therefore for low coverages we write

$$q(\theta) = q_0 - A\theta, \tag{9}$$

where A $(= -dq/d\theta)$ is a constant. By inserting Eq. (9) into (8) and (7) and taking $\Delta S_j = 0$ we get

$$\begin{aligned} D(\theta) = {} & \nu\lambda^2[1 + \theta(1 - \theta)A/kT] \\ & \times \exp\{[\theta(1 - \theta)A]/[kT + \theta(1 - \theta)A]\} \\ & \times \exp(-E_d/kT), \end{aligned} \tag{10}$$

where the first term in the square brackets is the thermodynamic factor multiplied by $(1 - \theta)$ and the first exponential term is due to the average lowering of the saddle point along the concentration gradient. For θ approaching zero for $A = 0$ (heat of adsorption constant) Eq. (10) reduces to Eq. (5). As the coverage increases it is the $\theta(1 - \theta)$ term in the thermodynamic factor that changes most, so that $D(\theta)$ approximates the form derived from the Boltzmann-Matano analysis of a linear diffusion profile. It is interesting to compare the terms in Eq. (10), derived by assuming $dq/d\theta$ to be constant, with those obtained from the Bragg-Williams lattice gas model [3]. This model considers only nearest neighbor interactions, of energy ϵ, and z nearest neighbor sites occupied. The thermodynamic factor and the term describing the lowering of the saddle point are identical if $A = z\epsilon$. This similarity is due to the fact that the Bragg-Williams model implicitly assumes, on average, a linear change in interaction energy with coverage.

Comparisons have been made between the values of $D(\theta)$ obtained by (a) analyzing the experimental results using the Boltzmann-Matano analysis of a straight line profile [Eq. (4)] with $\theta_1 = \frac{1}{12}$ ML and using Δx from the experimental profiles; and (b) the thermodynamic predictions of Eq. (10). Figure 4 shows the experimentally determined values obtained by analyzing the wings of diffusion profiles produced at $T = 333$, 348, and 363 K. It is assumed that diffusion is occurring primarily from the $\frac{1}{6}$ ML phase and the results are shown for concentrations below $\frac{1}{12}$ ML since the profile is complicated by the presence of the more condensed phase at higher θ. In order to compare these results with those derived from Eq. (10) we take $\nu = 10^{13}$ Hz, $\lambda = 3.84 \times 10^{-10}$ m, $A = 2$ eV/ML. This value of A gives an excellent fit to the shape of $D(\theta)$ at all three temperatures. The experimental value of $D(\theta)$ at $\theta = \frac{1}{12}$ ML is reproduced if values of $E_d = 0.51$, 0.47, and 0.47 eV are chosen for diffusion at 333, 348, and 363 K, respectively. At $\theta = 0$ the Boltzmann-Matano analysis of a straight line profile gives $D(0) = 0$ while the thermodynamic analysis gives the diffusion coefficient for single adatoms. There is good agreement between the experimental and theoretical curves with the single parameter, E_d, which is therefore determined to be close to 0.47 eV. A different choice of $(\nu\lambda^2)$ by a factor of 5, would change the value of E_d by ±0.05 eV.

To obtain straight line diffusion profiles, certain criteria have to be met. For $dq/d\theta$ to be constant there should be no stable phases over the θ range examined. This will usually mean that low concentrations are required, but that nevertheless adsorbate interactions are not negligible. This requires adsorbate systems with strong long range interactions and experimental techniques capable of measuring small concentrations accurately. Our b-SEI method has demonstrated this ability. It is interesting to note that the form $\theta(1 - C\theta)$ indicates particle-hole symmetry so linear diffusion profiles may also occur at higher coverages. Preliminary work on modeling these effects in detail using coupled rate and diffusion equations [5,14] show that such a model can be used to reproduce the main feature of the observed diffusion profiles.

We are grateful for SERC funding and one of us (M. A.) thanks the Government of the Islamic Republic of Pakistan for financial support.

---

*Also at Department of Physics and Astronomy, Arizona State University, Tempe, AZ 85287.

[1] D. A. King, J. Vac. Sci. Technol. **17**, 241 (1980).
[2] A. G. Naumovets and Yu S. Vedula, Surf. Sci. Rep. **4**, 365 (1985).
[3] R. Gomer, Rep. Prog. Phys. **53**, 917 (1990).
[4] M. Futamoto, M. Hanbucken, C. J. Harland, and J. A. Venables, Surf. Sci. **150**, 430 (1985).
[5] M. Azim, C. J. Harland, T. J. Martin, R. H. Milne, and J. A. Venables, Scanning Mic. **7**, 1153 (1993); M. Azim, R. H. Milne, R. Persaud, and J. A. Venables, Inst. Phys. Conf. Ser. **138**, 197 (1993); M. Azim, D.Phil thesis Sussex University (unpublished).
[6] M. Tikhov, G. Boishin, and L. Surnev, Surf. Sci. **241**, 103 (1991).
[7] *Physics and Chemistry of Alkali Metal Adsorption,* edited by H. P. Bonzel, A. M. Bradshaw, and G. Ertl (Elsevier, Amsterdam, 1989).
[8] N. D. Lang, Phys. Rev. B **4**, 4234 (1971).
[9] A. J. Smith, W. R. Graham, and E. W. Plummer, Surf. Sci. Lett. **243**, L37 (1991).
[10] T. Abukawa, T. Okane, and S. Kono, Surf. Sci. **256**, 370 (1991).
[11] H. Ishida, N. Shima, and M. Tsukada, Surf. Sci. **158**, 438 (1985).
[12] D. A. Reed and G. Ehrlich, Surf. Sci. **102**, 588 (1981); **105**, 603 (1981).
[13] A. G. Fedorus and A. G. Naumovets, Surf. Sci. **21**, 426 (1970).
[14] J. A. Venables, R. Persaud, F. L. Metcalfe, R. H. Milne, and M. Azim (to be published).